Slab flattening trigger for isotopic disturbance and magmatic flare-up in the southernmost Sierra Nevada batholith, California

Alan D. Chapman*, Jason B. Saleeby, and John Eiler
Division of Geological and Planetary Sciences, California Institute of Technology, 1200 E. California Boulevard, Pasadena, California 91125, USA

ABSTRACT

The San Emigdio Schist of Southern California permits examination of partial melting and devolatilization processes along a Late Cretaceous shallow subduction zone. Detrital and recrystallized zircon of the structurally highest portions of the schist bracket the depositional age to between ca. 102 and 98 Ma. Zircon oxygen isotope data from both lower-plate schist and upper-plate assemblages of the Sierra Nevada batholith (SNB) reveal a δ^{18}O shift of ~1.5‰ between igneous (~5.5‰) and recrystallized (~7‰) domains. These results, taken with previous zircon and whole-rock δ^{18}O measurements, provide evidence for devolatilization and/or partial melting of the schist and fluid ascent through overlying southwestern SNB upper-plate assemblages. Furthermore, the timing of mobile phase–rock interaction in the southwestern SNB is coincident with voluminous S-type magmatism in the southeastern SNB. We posit that during flattening of the Farallon slab, the schist was emplaced into the root zone of the southeastern SNB, where ensuing partial melting triggered a magmatic flare-up. Shallow subduction of the Cocos plate beneath central Mexico represents a close modern analog to this model.

INTRODUCTION

Continental arc magmatism is widely regarded to reflect melting of the mantle wedge by addition of fluids produced through metamorphism of trench sediments and oceanic crust in moderately to steeply dipping subduction zones (e.g., Bebout, 1991). In contrast, shallow subduction is commonly invoked to explain the termination and/or migration of arc magmatism (Dumitru et al., 1991; Saleeby, 2003). However, during slab flattening, subduction accretion assemblages may be transported into the magmatic source region of an active arc. Subsequent partial melting of fertile underplated material may trigger a brief episode of high-flux magmatism prior to arc shutoff. This study focuses on the spatial and temporal association of slab shallowing and magmatic flare-up in the Sierra Nevada batholith (SNB) of California to better understand how supracrustal rocks are emplaced into continental arc source regimes and how the input of these materials influences magma productivity and composition.

We present here new and published in situ zircon U-Pb and oxygen isotope data to better understand aqueous fluid– and/or partial melt (i.e., mobile phase)–rock interaction accompanying Late Cretaceous shallow subduction of the Farallon plate beneath North America. Data presented herein lead us to suggest that devolatilization and/or partial melting of underplated subduction assemblages altered the isotopic composition of, and triggered a magmatic flare-up in, the SNB. We make the case that "relamination" of subducted material to the base of the arc crust (Hacker et al., 2011; Behn et al., 2011) drove copious magmatism and the generation of S-type granitoids in the southern SNB.

*Department of Geological Sciences and Engineering, Missouri University of Science and Technology, 129 McNutt Hall, 1400 N. Bishop Ave, Rolla, MO 65409, USA; E-mail: chapmanad@mst.edu.

SOUTHERN SIERRA NEVADA BATHOLITH

Late Cretaceous to early Tertiary shallow subduction beneath the formerly (pre–San Andreas fault) contiguous southern SNB–Salinia–Mojave Desert region resulted in major lithospheric reorganization, associated with tectonic removal of subcontinental mantle and replacement with accretionary wedge and/or forearc basin material (e.g., Saleeby, 2003). These subduction accretion assemblages, known locally as the Pelona-Orocopia-Rand schist (Jacobson et al., 2011), lie in fault contact beneath the SNB and its pre-intrusive framework (Fig. 1). Exposures of these rocks in the San Emigdio Mountains (the "San Emigdio Schist") are juxtaposed beneath deeply exhumed, ca. 100–135 Ma, mafic to intermediate batholithic (referred to below as "western domain") rocks along the Rand fault, a Late Cretaceous low-angle normal shear zone that remobilized the shallow subduction megathrust (Chapman et al., 2010). Numerous Late Cretaceous shear zones separate western-domain rocks from a distinct "eastern domain" made up of shallow to mid-crustal, ca. 85–100 Ma, intermediate to felsic S-type plutons (Miller et al., 1996).

The San Emigdio Schist exhibits an upsection increase in metamorphic grade with evidence for fluid-saturated partial melting and extensive fluid flow restricted to shallow structural levels (<100 m from the Rand fault) of the exposure (Chapman et al., 2011). These features have been explained, in this and related schists, by a combination of shear heating along the subduction interface (Graham and England, 1976; Ducea et al., 2009) and tectonic underplating and progressive cooling beneath an initially hot upper plate following the onset of shallow subduction (Kidder and Ducea, 2006; Chapman et al., 2011; Kidder et al., 2013).

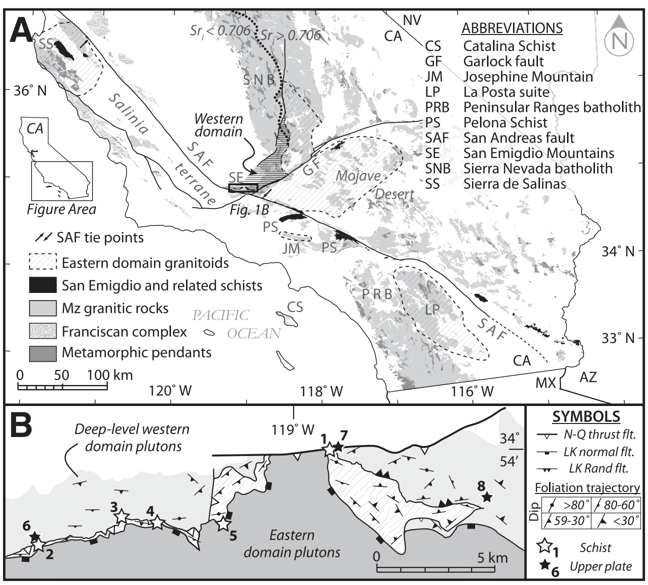

Figure 1. Geologic maps compiled by Chapman et al. (2011) showing southern California basement rocks (A) and sample locations (numbered stars) in the San Emigdio Mountains (B). Schist is shown in white in B. NV—Nevada; CA—California; AZ—Arizona; MX—Mexico; Mz—Mesozoic; N-Q—Neogene-Quaternary; LK—Late Cretaceous.

GEOLOGY, September 2013; v. 41; no. 9; p. 1007–1010; Data Repository item 2013281 | doi:10.1130/G34445.1 | Published online 11 July 2013

RESULTS

U-Pb detrital zircon geochronology was conducted on three new samples of the San Emigdio Schist (see the GSA Data Repository[1]) and integrated with existing data of Grove et al. (2003) and Jacobson et al. (2011). Sample depths (Fig. 2) were approximated based on the structural distance from the Rand fault and metamorphic grade. All samples exhibit (1) a major mid- to Late Cretaceous age peak with scattered Early Cretaceous, Jurassic, and Triassic ages, and rare pre-Mesozoic grains, and (2) maximum depositional ages of ca. 100 Ma, calculated from the three youngest zircon grains in each sample that overlap in age within error and exhibit oscillatory zoning. Zircon grains from samples collected >100 m from the Rand fault are characterized by simple oscillatory zoning and are interpreted to be detrital. Within ~100 m of the Rand fault, zircon grains exhibit 1–50-µm-thick cathodoluminescence (CL)-bright rims with complex zonation features that cross cut detrital cores. Such rims were not observed at deeper structural levels. Relative to less disturbed grains, these recrystallized domains are younger (ca. 99–91 Ma), with generally higher U concentration (2411–3197 ppm), U-Th ratios (generally >10; Fig. 2), and $\delta^{18}O$ values (see below; Fig. 3). This 99–91 Ma age range likely reflects the timing of peak metamorphism of the schist. Similar overgrowths are reported from the related schist of Sierra de Salinas (Barth et al., 2003).

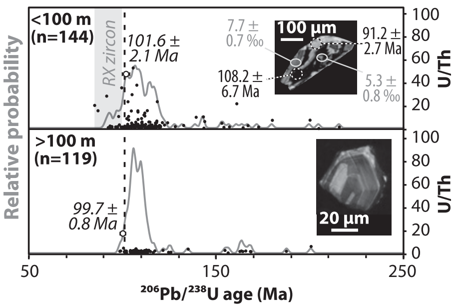

Figure 2. U-Pb detrital zircon age spectra, U/Th values, and representative cathodoluminescence (CL) images from San Emigdio Schist. Circles and ellipses in upper CL image indicate analyzed areas labeled with $^{206}Pb/^{238}U$ ages and $\delta^{18}O$ values, respectively. Curves are composites of samples located <100 m (Fig. 1, samples 1, 2, and 3; image from sample 1) and >100 m (Fig. 1, samples 4 and 5; image from sample 5) from the Rand fault. Open circles (2σ error bars; connected by dashed lines) denote weighted averages of the three youngest detrital grains, excluding recrystallized domains, in each group. Sample 2 is from Grove et al. (2003), samples 3 and 4 are from Jacobson et al. (2011), and the remainder are from this study. RX—recrystallized. Isotopic data are provided in Table DR1 (see footnote 1).

Zircon grains from western-domain plutonic assemblages within 100 m of the Rand fault exhibit oscillatory zoned, ca. 135 Ma cores mantled by CL-homogenous, ca. 103–98 Ma rims with elevated U concentrations and U-Th ratios (Chapman et al., 2012). Oxygen isotope ratios were determined (see the Data Repository) from a subset of schist and upper-plate zircons also studied by U-Pb geochronology (Fig. 3). Measured $\delta^{18}O$ from schist and upper-plate zircon cores average 5.61‰ ± 0.33‰ and 5.37‰ ± 0.20‰, respectively. Values of $\delta^{18}O$ from recrystallized domains in the same grains yield a weighted mean of 7.20‰ ± 0.46‰ (schist) and 6.96‰ ± 0.63‰ (upper plate).

UPPER PLATE ISOTOPIC MODIFICATION

The abundance of mid- to Late Cretaceous detrital zircon grains reported here is consistent with previous interpretations (Grove et al., 2003; Jacobson et al., 2011) that the sedimentary protoliths of the San Emigdio Schist were first-cycle clastic deposits sourced from the western to central SNB. Throughout the schist section, the youngest demonstrably detrital grain clusters are identical in age (ca. 100 Ma), within analytical error (Fig. 2). The recrystallization of zircon between ca. 99 and 91 Ma within ~100 m of the Rand fault is likely due to emplacement of this structurally highest material beneath hot (680–790 °C; Pickett and Saleeby, 1993; Chapman et al., 2011) upper-plate rocks. By this interpretation, the depositional age of the structurally highest portions of the San Emigdio Schist is bracketed to the time interval between the youngest detrital U-Pb zircon ages (ca. 101 Ma) and the timing of peak metamorphism (ca. 99–91 Ma).

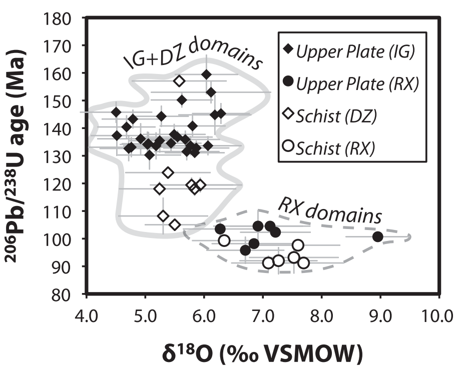

Figure 3. Relationship between $^{206}Pb/^{238}U$ age and $\delta^{18}O$ values for upper-plate and schist zircon. Domains: IG—igneous; RX—recrystallized; DZ—detrital. VSMOW—Vienna standard mean ocean water. Errors are 2σ.

Zircon core $\delta^{18}O$ values of 5.3‰ ± 0.3‰ in both the San Emigdio Schist and upper-plate plutonic assemblages suggest limited input of supracrustal material during igneous crystallization (e.g., Lackey et al., 2005). Values of $\delta^{18}O$ measured from recrystallized domains in upper-plate and schist zircon are ~1.5‰ higher than those of oscillatory-zoned regions in the same grains, suggesting that zircon recrystallization occurred in the presence of an isotopically heavy melt and/or aqueous fluid phase. This mobile phase was at least in part schist derived, based on evidence for in situ veining, partial melting, and devolatilization associated with prograde metamorphism (Chapman et al., 2011). However, schist whole-rock (WR) $\delta^{18}O$ values of 9.9‰–19.5‰ (Ross, 1989; Miller et al., 1996) are significantly higher than zircon rim values of 7.20‰ ± 0.46‰, suggesting that mixing of schist-derived mobile phases with those with relatively low $\delta^{18}O_{WR}$, such as unaltered mid-oceanic-ridge basalt may have taken place.

Elevated upper-plate zircon (Zr) $\delta^{18}O$ values are spatially and temporally related to schist emplacement. Lackey et al. (2005) reported $\delta^{18}O_{Zr}$ values of 7.8‰ ± 0.7‰ from deeply exhumed ca. 83–117 Ma plutonic rocks of the southernmost SNB, and lower values of 6.1‰ ± 0.9‰ from shallower-level assemblages of similar age and composition from the central SNB. Furthermore, Lackey et al. (2005) noted an increase in $\delta^{18}O_{Zr}$ values from ~7.4‰ to 8.3‰ at ca. 100 Ma in both eastern- and western-domain plutons, consistent with our observation of young (96–105 Ma) overgrowths with elevated $\delta^{18}O$ on old (ca. 135 Ma) upper-plate zircon cores, and attribute this change to a greater supracrustal input with time. Assimilation of high-$\delta^{18}O$ metamorphic framework rocks may account for localized contamination of plutons in the southernmost SNB, but cannot explain the pervasive shift toward higher $\delta^{18}O_{Zr}$ at ca. 100 Ma. We propose that partial melting and/or devolatilization of the earliest-formed San Emigdio Schist at ca. 100 Ma led to metamorphism and isotopic contamination of western-domain upper-plate plutonic assemblages (Fig. 4). Emplacement of Late Cretaceous eastern-domain isotopically anomalous plutons younger than ca. 100 Ma are likewise explained by the model discussed below.

RELATION OF SCHIST UNDERPLATING TO VOLUMINOUS ARC MAGMATISM

Our age constraints indicate that the San Emigdio Schist was subducted to 30–35 km depth (Chapman et al., 2011) between 100 and 90 Ma. Therefore, it is likely that subduction accretion assemblages were present beneath

[1]GSA Data Repository item 2013281, analytical techniques, sample petrography, isotopic data, and additional cathodoluminescence images, is available online at www.geosociety.org/pubs/ft2013.htm, or on request from editing@geosociety.org or Documents Secretary, GSA, P.O. Box 9140, Boulder, CO 80301, USA.

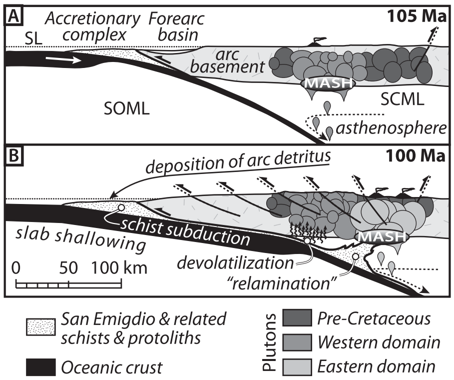

Figure 4. Generalized cross-section model for the southern Sierra Nevada batholith. No vertical exaggeration. A: Ca. 105 Ma eastward subduction of Farallon plate beneath North America prior to shallow subduction. B: Ca. 100 Ma slab shallowing (due to subduction of thickened oceanic crust; Saleeby, 2003) and schist deposition, subduction, devolatilization (western domain), and diapiric rise and relamination (eastern domain). MASH—zone of melting, assimilation, storage, and homogenization; SCML—subcontinental mantle lithosphere; SL—sea level; SOML—sub-oceanic mantle lithosphere.

the southern SNB–Salinia–Mojave Desert region during emplacement of eastern-domain ca. 92–85 Ma S-type granitoids (Fig. 1). Plutons within this belt were likely derived from a source rich in immature clastic sediments, based on elevated $\delta^{18}O_{WR}$ (10.6‰ ± 1.6‰) and initial $^{87}Sr/^{86}Sr$ (Sr_i; 0.7077 ± 0.0011) and negative ε_{Nd} (–6.0 ± 2.2; Ross, 1989; Miller et al., 1996; Kistler and Champion, 2001). These isotopic relations and the paucity of metasedimentary rocks in these plutons preclude regional-scale assimilation of these assemblages as the source for this cryptic imprint.

Instead, we suggest that the San Emigdio and related schists were emplaced into the melting, assimilation, storage, and homogenization (MASH; Hildreth and Moorbath, 1988) zone of the Sierran arc during slab flattening. Partial melting in the relaminated schist is hypothesized to have taken place within the magmatic source region to produce S-type granitoids in the eastern domain (Fig. 4). The emplacement of S-type granitoids in the southernmost SNB and adjacent areas occurred during eastward arc migration and at the peak of a ca. 100–85 Ma high-magmatic-flux event (Ducea, 2001). Magmatic flare-ups are thought to be triggered by supracrustal input, either by subduction erosion from the trench side or retroarc thrusting from the foreland (Ducea, 2001; Ducea and Barton, 2007). Ducea (2001) invoked east-vergent thrusting of the arc over North American continental lithosphere to explain magmatic flare-ups for the entire length of the SNB. This argument is bolstered by 100–85 Ma plutons north of ~36°N with $\delta^{18}O_{Zr}$ values of ~6.5‰ at Sr_i ~0.706–0.707 (Kistler, 1990; Lackey et al., 2008). However, south of ~36°N, $\delta^{18}O_{Zr}$ values are ~1.7‰ higher at similar Sr_i (Saleeby et al., 1987; Kistler, 1990; Pickett and Saleeby, 1994; Miller et al., 1996; Lackey et al., 2005), reflecting a higher proportion of supracrustal material to crystalline basement as a source component. Furthermore, there is little evidence for major Late Cretaceous deformation along the Cordilleran retroarc thrust belt south of ~36°N (e.g., DeCelles, 2004) and this latitude corresponds to the inferred northern limit of shallow subduction (Saleeby, 2003). Therefore, 100–85 Ma high-flux magmatism must be related to fundamentally different processes north (retroarc thrusting) and south (shallow subduction and dehydration melting of underplated schist) of ~36°N.

Arc magmatism ceased throughout the SNB between ca. 80 and 85 Ma (e.g., Chen and Moore, 1982). Shallow subduction and the removal of mantle lithosphere from beneath the southern SNB–Salinia–Mojave Desert region cannot account for the shutoff of magmatism in the greater SNB, where the mantle wedge was left intact (Saleeby et al., 2003). Ducea (2001) suggested that the mantle lithosphere and lower crust of the central and northern SNB became melt drained and infertile following Late Cretaceous retroarc thrusting and associated magmatism. This study suggests, however, that the cessation of magmatism south of ~36°N must have been related to a different process. A hybrid model of melt suppression due to disruption of asthenospheric circulation patterns by shallow subduction (e.g., Barazangi and Isacks, 1976) in the southern SNB and concomitant melt depletion of the retroarc source region in the central and northern SNB provides one explanation for the cessation of magmatism throughout the greater SNB between ca. 80 and 85 Ma. Alternatively, arc shutoff may simply be related to large-scale disruption of asthenospheric circulation patterns by shallow subduction in the southern SNB and adjacent areas (Saleeby, 2003).

POSSIBLE ANALOGS

The isotopic and structural relations exhibited by Late Cretaceous granitoids in the southern SNB are strikingly similar to those of the ca. 98–92 Ma La Posta plutonic suite in the northernmost Peninsular Ranges batholith (Fig. 1; Kistler et al., 2003). The La Posta suite is underlain by the Catalina Schist, a mid- to Late Cretaceous subduction complex exhibiting evidence for upward migration of fluids and isotopic contamination of structurally high units (Bebout, 1991). These relations led Grove et al. (2008) to hypothesize that subduction erosion delivered the Catalina Schist to the magmatic source, causing partial melting and/or devolatilization in the schist and igniting a magmatic flare-up in the northernmost Peninsular Ranges batholith. Likewise, granitoids with Sr_i > 0.708, $\delta^{18}O_{WR}$ > 8.6‰, and ε_{Nd} < –10 of the ca. 72–86 Ma Josephine Mountain intrusion of the San Gabriel Mountains (Fig. 1; Barth et al., 1995) overlap in age with the youngest zircons (ca. 79–82 Ma) at high structural levels of the underlying Pelona schist (Grove et al., 2003), suggesting a possible schist source component for the intrusion.

Shallow subduction of the Cocos plate beneath central Mexico may be the best modern analog to the model presented in Figure 4. Unlike other modern examples of shallow subduction, arc magmatism is still active above the downgoing Cocos plate (e.g., Gómez-Tuena et al., 2007). The Cocos plate underthrusts the base of the crust horizontally at ~50 km, where a thin (~10 km) ultralow-velocity layer intervenes (Pérez-Campos et al., 2008). This layer is thought to comprise a mixture of hydrated mantle wedge, altered oceanic crust, and tectonically eroded forearc material (Keppie et al., 2012). Therefore, it is conceivable that incorporation of forearc material at the base of the arc facilitated andesitic volcanism above the Cocos plate.

SUMMARY AND OUTLOOK

Combined zircon U-Pb and oxygen isotopic data lead us to hypothesize that subduction accretion assemblages may be emplaced into continental arc source regimes during slab shallowing, leading to brief (<10 m.y.) episodes of high-flux magmatism. Further evaluation of this hypothesis can come from geochronologic, geochemical, and isotopic analysis of upper-plate and lower-plate rocks in exhumed shallow subduction systems (e.g., the North Cascades crystalline core, Washington; Matzel et al., 2004) or from geochemical and/or geophysical investigation of modern systems.

ACKNOWLEDGMENTS

This research was supported by National Science Foundation grant EAR- 0739071 awarded to Saleeby. This is Caltech Tectonics Observatory contribution number 222. We thank Yunbin Guan for analytical assistance; Rita Economos, Sue Kay, Sarah Roeske, and Luigi Solari for insightful reviews; Rónadh Cox and Sandra Wyld for editorial handling; and Paul Asimow, Carl Jacobson, and Steven Kidder for discussions.

REFERENCES CITED

Barazangi, M., and Isacks, B., 1976, Spatial distribution of earthquakes and subduction of the Nazca plate beneath South America: Geology, v. 4, p. 686–692, doi:10.1130/0091-7613(1976)4<686:SDOEAS>2.0.CO;2.

Barth, A.P., Wooden, J.L., Tosdal, R.M., and Morrison, J., 1995, Crustal contamination in the petrogenesis of a calc-alkalic rock series: Josephine Mountain intrusion, California: Geological Society of America Bulletin, v. 107, p. 201–212, doi:10.1130/0016-7606(1995)107<0201:CCITPO>2.3.CO;2.

Barth, A.P., Wooden, J.L., Grove, M., Jacobson, C.E., and Pedrick, J.N., 2003, U-Pb zircon geochronology of rocks in the Salinas Valley region of California: A reevaluation of the crustal structure and origin of the Salinian block: Geology, v. 31, p. 517–520, doi:10.1130/0091-7613(2003)031<0517:UZGORI>2.0.CO;2.

Bebout, G.E., 1991, Field-based evidence for devolatilization in subduction zones: Implications for arc magmatism: Science, v. 251, p. 413–416, doi:10.1126/science.251.4992.413.

Behn, M.D., Kelemen, P.B., Hirth, G., Hacker, B.R., and Massonne, H.-J., 2011, Diapirs as the source of the sediment signature in arc lavas: Nature Geoscience, v. 4, p. 641–646, doi:10.1038/ngeo1214.

Chapman, A.D., Kidder, S., Saleeby, J.B., and Ducea, M.N., 2010, Role of extrusion of the Rand and Sierra de Salinas schists in Late Cretaceous extension and rotation of the southern Sierra Nevada and vicinity: Tectonics, v. 29, TC5006, doi:10.1029/2009TC002597.

Chapman, A.D., Luffi, P., Saleeby, J., and Petersen, S., 2011, Metamorphic evolution, partial melting, and rapid exhumation above an ancient flat slab: Insights from the San Emigdio Schist, southern California: Journal of Metamorphic Geology, v. 29, p. 601–626, doi:10.1111/j.1525-1314.2011.00932.x.

Chapman, A.D., Saleeby, J.B., Wood, D.J., Piasecki, A., Farley, K.A., Kidder, S., and Ducea, M.N., 2012, Late Cretaceous gravitational collapse of the southern Sierra Nevada batholith, California: Geosphere, v. 8, p. 314–341, doi:10.1130/GES00740.1.

Chen, J.H., and Moore, J.G., 1982, Uranium-lead isotopic ages from the Sierra Nevada batholith, California: Journal of Geophysical Research, v. 87, p. 4761–4784, doi:10.1029/JB087iB06p04761.

DeCelles, P.G., 2004, Late Jurassic to Eocene evolution of the Cordilleran thrust belt and foreland basin system, western U.S.A.: American Journal of Science, v. 304, p. 105–168, doi:10.2475/ajs.304.2.105.

Ducea, M., 2001, The California arc: Thick granitic batholiths, eclogitic residues, lithospheric-scale thrusting, and magmatic flare-ups: GSA Today, v. 11, no. 11, p. 4–10, doi:10.1130/1052-5173(2001)011<0004:TCATGB>2.0.CO;2.

Ducea, M.N., and Barton, M.D., 2007, Igniting flare-up events in Cordilleran arcs: Geology, v. 35, p. 1047–1050, doi:10.1130/G23898A.1.

Ducea, M.N., Kidder, S., Chesley, J.T., and Saleeby, J.B., 2009, Tectonic underplating of trench sediments beneath magmatic arcs: The central California example: International Geology Review, v. 51, p. 1–26.

Dumitru, T.A., Gans, P.B., Foster, D.A., and Miller, E.L., 1991, Refrigeration of the western Cordilleran lithosphere during Laramide shallow-angle subduction: Geology, v. 19, p. 1145–1148, doi:10.1130/0091-7613(1991)019<1145:ROTWCL>2.3.CO;2.

Gómez-Tuena, A., Orozco-Esquivel, M.T., and Ferrari, L., 2007, Igneous petrogenesis of the Trans-Mexican Volcanic Belt, *in* Alaniz-Alvarez, S.A., and Nieto-Samaniego, A.F., eds., Geology of México: Celebrating the Centenary of the Geological Society of México: Geological Society of America Special Paper 422, p. 129–181, doi:10.1130/2007.2422(05).

Graham, C.M., and England, P.C., 1976, Thermal regimes and regional metamorphism in the vicinity of overthrust faults: An example of shear heating and inverted metamorphic zonation from southern California: Earth and Planetary Science Letters, v. 31, p. 142–152, doi:10.1016/0012-821X(76)90105-9.

Grove, M., Jacobson, C.E., Barth, A.P., and Vucic, A., 2003, Temporal and spatial trends of Late Cretaceous–early Tertiary underplating Pelona and related schist beneath southern California and southwestern Arizona, *in* Johnson, S.E., et al., eds., Tectonic Evolution of Northwestern Mexico and the Southwestern USA: Geological Society of America Special Paper 374, p. 381–406, doi:10.1130/0-8137-2374-4.381.

Grove, M., Bebout, G.E., Jacobson, C.E., Barth, A.P., Kimbrough, D.L., King, R.L., Zou, H., Lovera, O.M., Mahoney, B.J., and Gehrels, G.E., 2008, The Catalina Schist: Evidence for Middle Cretaceous subduction erosion of southwestern North America, *in* Draut, A.E., Clift, P.D., and Scholl, D.W., eds., Formation and Applications of the Sedimentary Record in Arc Collision Zones: Geological Society of America Special Paper 436, p. 335–361, doi:10.1130/2008.2436(15).

Hacker, B.R., Kelemen, P.B., and Behn, M.D., 2011, Differentiation of the continental crust by relamination: Earth and Planetary Science Letters, v. 307, p. 501–516, doi:10.1016/j.epsl.2011.05.024.

Hildreth, W., and Moorbath, S., 1988, Crustal contributions to arc magmatism in the Andes of central Chile: Contributions to Mineralogy and Petrology, v. 98, p. 455–489, doi:10.1007/BF00372365.

Jacobson, C.E., Grove, M., Pedrick, J.N., Barth, A.P., Marsaglia, K.M., Gehrels, G.E., and Nourse, J.A., 2011, Late Cretaceous–early Cenozoic tectonic evolution of the southern California margin inferred from provenance of trench and forearc sediments: Geological Society of America Bulletin, v. 123, p. 485–506, doi:10.1130/B30238.1.

Keppie, D.F., Hynes, A.J., Lee, J.K.W., and Norman, M., 2012, Oligocene–Miocene back-thrusting in southern Mexico linked to the rapid subduction erosion of a large forearc block: Tectonics, v. 31, TC2008, doi:10.1029/2011TC002976.

Kidder, S., and Ducea, M.N., 2006, High temperatures and inverted metamorphism in the schist of Sierra de Salinas, California: Earth and Planetary Science Letters, v. 241, p. 422–437, doi:10.1016/j.epsl.2005.11.037.

Kidder, S.B., Herman, F., Saleeby, J., Avouac, J.-P., Ducea, M.N., and Chapman, A.D., 2013, Shear heating not a cause of inverted metamorphism: Geology, v. 41, p. 899–902, doi: 10.1130/G34289.1.

Kistler, R.W., 1990, Two different lithosphere types in the Sierra Nevada, California, *in* Anderson, J.L., ed., The Nature and Origin of Cordilleran Magmatism: Geological Society of America Memoir 174, p. 271–281.

Kistler, R.W., and Champion, D.E., 2001, Rb-Sr whole-rock and mineral ages, K-Ar, $^{40}Ar/^{39}Ar$, and U-Pb mineral ages, and strontium, lead, neodymium, and oxygen isotopic compositions for granitic rocks from the Salinian Composite Terrane, California: U.S. Geological Survey Open-File Report 01-453, 84 p.

Kistler, R.W., Wooden, J.L., and Morton, D.M., 2003, Isotopes and ages in the northern Peninsular Ranges batholith, southern California: U.S. Geological Survey Open-File Report 03-489, 45 p.

Lackey, J.S., Valley, J.W., and Saleeby, J.B., 2005, Supracrustal input to magmas in the deep crust of Sierra Nevada batholith: Evidence from high-$\delta^{18}O$ zircon: Earth and Planetary Science Letters, v. 235, p. 315–330, doi:10.1016/j.epsl.2005.04.003.

Lackey, J.S., Valley, J.W., Chen, J.H., and Stockli, D.F., 2008, Dynamic magma systems, crustal recycling, and alteration in the central Sierra Nevada batholith: The oxygen isotope record: Journal of Petrology, v. 49, p. 1397–1426, doi:10.1093/petrology/egn030.

Matzel, J.P., Bowring, S.A., and Miller, R.B., 2004, Protolith age of the Swakane Gneiss, North Cascades, Washington: Evidence of rapid underthrusting of sediments beneath an arc: Tectonics, v. 23, TC6009, doi:10.1029/2003TC001577.

Miller, J.S., Glazner, A.F., and Crowe, D.E., 1996, Muscovite-garnet granites in the Mojave Desert: Relation to crustal structure of the Cretaceous arc: Geology, v. 24, p. 335–338, doi:10.1130/0091-7613(1996)024<0335:MGGITM>2.3.CO;2.

Pérez-Campos, X., Kim, Y., Husker, A., Davis, P.M., Clayton, R.W., Iglesias, A., Pacheco, J.F., Singh, S.K., Manea, V.C., and Gurnis, M., 2008, Horizontal subduction and truncation of the Cocos Plate beneath central Mexico: Geophysical Research Letters, v. 35, L18303, doi:10.1029/2008GL035127.

Pickett, D.A., and Saleeby, J.B., 1993, Thermobarometric constraints on the depth of exposure and conditions of plutonism and metamorphism at deep levels of the Sierra Nevada Batholith, Tehachapi Mountains, California: Journal of Geophysical Research, v. 98, p. 609–629, doi:10.1029/92JB01889.

Pickett, D.A., and Saleeby, J.B., 1994, Nd, Sr, and Pb isotopic characteristics of Cretaceous intrusive rocks from deep levels of the Sierra Nevada batholith, Tehachapi Mountains, California: Contributions to Mineralogy and Petrology, v. 118, p. 198–215, doi:10.1007/BF01052869.

Ross, D.C., 1989, The metamorphic and plutonic rocks of the southernmost Sierra Nevada, California, and their tectonic framework: U.S. Geological Survey Professional Paper 1381, 159 p.

Saleeby, J., 2003, Segmentation of the Laramide slab: Evidence from the southern Sierra Nevada region: Geological Society of America Bulletin, v. 115, p. 655–668, doi:10.1130/0016-7606(2003)115<0655:SOTLSF>2.0.CO;2.

Saleeby, J.B., Sams, D.B., and Kistler, R.W., 1987, U/Pb zircon, strontium, and oxygen isotopic and geochronological study of the southernmost Sierra Nevada Batholith, California: Journal of Geophysical Research, v. 92, p. 10,443–10,466, doi:10.1029/JB092iB10p10443.

Saleeby, J.B., Ducea, M.N., and Clemens-Knott, D., 2003, Production and loss of high-density batholithic root, southern Sierra Nevada, California: Tectonics, v. 22, 1064, doi:10.1029/2002TC001374.

Manuscript received 4 February 2013
Revised manuscript received 7 May 2013
Manuscript accepted 8 May 2013

Printed in USA